



ELSEVIER

Journal of Nuclear Materials 283–287 (2000) 987–991

**journal of
nuclear
materials**

www.elsevier.nl/locate/jnucmat

Ductility correlations between shear punch and uniaxial tensile test data

M.B. Toloczko ^{a,*}, M.L. Hamilton ^a, G.E. Lucas ^b^a Pacific Northwest National Laboratory, Richland, WA 99352, USA^b University of California, Santa Barbara, CA 93106, USA

Abstract

The shear punch test was developed to address the need of the fusion reactor structural materials community for small scale mechanical properties tests. It has been demonstrated that effective shear strength data obtained from the shear punch test can be linearly related to uniaxial tensile strength for a wide variety of alloys. The current work explores the existence of a similar relationship between shear punch test data and both the tensile strain hardening exponent and the uniform elongation. © 2000 Elsevier Science B.V. All rights reserved.

1. Introduction

Selection and development of fusion reactor first wall materials are partially guided by the mechanical properties of candidate first wall materials. Existing or proposed 14 MeV neutron sources for irradiated materials characterization have or will have a relatively small volume which places limitations on specimen size and geometry. TEM disk-based mechanical properties tests have been given serious consideration because of the small volume occupied by a TEM disk. The shear punch test is a TEM disk-based mechanical properties test that was developed to provide strength and ductility information [1].

In a shear punch test, a flat-ended cylindrical punch is used to punch a 1 mm diameter slug out of a TEM disk [2]. The load on the punch is measured as a function of the punch displacement. The shear punch load-displacement curve exhibits a linear elastic region that is followed by a region of plastic strain. The load eventually reaches a maximum and then declines until the specimen fails.

During a shear punch test, the stress state in the deformation region is known to contain both shear and normal stress components [3]. In a cylindrical coordinate system with the punch axis defining the z -axis, the effective shear stress in the specimen is defined by assuming that the rz shear stress in the deformation region supports the entire load placed on the specimen. Thus, the equation for the effective shear stress is

$$\tau = \frac{P}{2\pi r t}, \quad (1)$$

where P is the load on the punch, r the average of the punch and die radii, and t is the specimen thickness. The effective shear yield stress is taken from the load at deviation from linearity in the shear punch load vs. displacement trace. The effective shear ultimate stress is taken from the maximum load obtained during a test.

In the original shear punch work [1] and in a later work [2], a linear correlation was observed between uniaxial yield stress from tensile tests and effective shear yield stress. A linear correlation was also observed between uniaxial ultimate stress from tensile tests and effective shear ultimate stress. The correlations can be fitted using the equation

$$s = m(\tau - \tau_0), \quad (2)$$

where s and τ refer to the engineering values of either the uniaxial yield stress and the effective shear yield stress or the uniaxial ultimate stress and the effective shear

* Corresponding author. Tel.: +1-509 376 0156; fax: +1-509 376 0418.

E-mail address: mychailo.toloczko@pnl.gov (M.B. Toloczko).

ultimate stress, respectively; τ_0 is a fitting coefficient with units of stress, and it represents the intercept of the linear correlation with the effective shear stress (horizontal) axis; m is also a fitting coefficient. It was found that the fitting coefficients are different for the yield and ultimate correlations.

The original work [1] also showed that a linear relationship exists between the measured tensile strain hardening exponent, n , and n_τ , a strain hardening exponent calculated from an equation containing the ratio of the effective shear ultimate stress to the effective shear yield stress, τ_m/τ_y . The equation for calculating n_τ is based on the equation

$$\left(\frac{n_\sigma}{0.002}\right)^{n_\sigma} = \frac{\sigma_m}{\sigma_y}, \quad (3)$$

where the ‘ σ ’ subscript denotes n_σ which is calculated from the ratio of tensile stresses. Eq. (3) is obtained by assuming power law strain hardening (PLSH). If PLSH is assumed, then $\sigma_y = k(0.002)^n$ and $\sigma_m = k(n)^n$. The ratio of these equations gives Eq. (3). n_τ was found by using τ_m/τ_y in place of σ_m/σ_y . Based on such an equation, a 1:1 relationship between n and n_τ was proposed by Lucas et al. [1], and the results of their work showed that within the range of $n \leq 0.20$, a 1:1 relationship did indeed exist. Lucas et al. also observed a 1:1 relationship between tensile reduction of area (RA) and shear punch displacement at failure, d_f/t .

The purpose of the current work is to further investigate the relationship between tensile ductility and ductility predicted from the shear punch test. Uniaxial tensile data and shear punch data from a variety of materials were used in the study. By using a wide variety of materials, it was possible to expand the range of ductility and strain hardening behavior compared to the original work of Lucas et al. Due to its impractical nature, reduction of area measurements was not per-

formed, and instead, emphasis was placed on exploring the relationship between τ_m/τ_y and n or ε_u .

2. Experimental procedure

2.1. Materials and specimen fabrication

Table 1 shows the materials and the thermomechanical treatments used in producing the sheet stock from which the specimens were fabricated. Sheet stock was nominally 0.25 mm (0.010 in.) in thickness. The aluminum alloy TEM disks were punched from sheet stock, while the other TEM disks were all electrodischarge machined (EDM). Aluminum alloy miniature tensile specimens were machined from sheet stock while the remainder of the miniaturized tensile specimens were cut from sheet stock by EDM. Two different tensile specimen geometries were utilized. The aluminum alloy tensile specimens had 30 mm \times 3 mm gauge dimensions while the remainder had 5 mm \times 1 mm gauge dimensions. Further information on specimen fabrication and thermomechanical treatments can be found in [4–8].

2.2. Testing

A shear punch fixture with a 1.00 mm diameter punch and 1.04 mm diameter receiving-hole was utilized for this experiment. Shear punch tests were performed at room temperature using a screw driven Instron load frame with crosshead speed set to either 1.67×10^{-3} or 2.12×10^{-3} mm/s. Crosshead displacement was measured during testing, and punch displacement was assumed to be equal to crosshead displacement. Load was monitored with a standard load cell. Ten shear punch tests were performed for each aluminum alloy/TMT combination, five shear punch tests were performed per

Table 1
Materials and TMTs used for this work

Alloy	Thermomechanical treatment	Tests/TMT	
		SP ^a	T ^b
5052	0 (Solution annealed), H38 (aged and CW)	10	3
6061	0 (Solution annealed), T6 (aged)	10	3
316	SA, 20% CW, 40% CW, 2 age/cw treatments	5	2
HT9	Normalized, 4 different tempering treatments	5	2
316, 316L	SA, CW	3	2
CuAl25	50% CW	3	2
MZC-3	Aged and cold-worked	3	2
CuHfO ₂	20% CW	3	2
V-5Cr-5Ti	950°C/1 h/furnace cool	3	3
V-3Ti-0.3Si	1150°C/1 h/furnace cool	3	3

^a Shear punch.

^b Tensile.

TMT for the US 316 SS and HT9 alloys, and two or three shear punch tests were performed for each of the remaining alloy/TMT combinations. The standard deviation in the measured effective shear yield stress was less than or equal to $\pm 10\%$ of the average value, while the standard deviation in the measured effective shear ultimate stress was less than or equal to $\pm 5\%$ of the average value. Further details on the shear punch testing can be found in [2,7].

The tensile tests were also performed at room temperature. Aluminum alloy specimens were tested on an Instron load frame. Displacement was measured with a linear variable differential transformer (LVDT), while load was measured with a standard load cell. The elongation rate was 0.1 mm/s ($3.3 \times 10^{-3} \text{ s}^{-1}$). Ten tests were performed for each aluminum alloy/TMT combination. Minimal data scatter was observed, and only data from three aluminum alloy specimens were examined per alloy/TMT combination. Further details on tensile testing of the aluminum alloys can be found in [8]. The remaining tensile specimens were tested on a horizontal frame [9]. Elongation of the gauge section was considered to be equal to crosshead displacement, while load was measured with a standard load cell. The elongation rate was $2 \times 10^{-3} \text{ mm/s}$ ($4 \times 10^{-4} \text{ s}^{-1}$). Two or three tests were done for each alloy/TMT combination.

2.3. Measurement of strain hardening exponent and true uniform elongation from the tensile tests

The strain hardening exponent, n , was determined from log–log plots of true stress (σ) vs. true plastic strain (ϵ_{pl}). It was observed that all the materials deviated from PLSH behavior to various degrees. Some typical traces are shown in Fig. 1. The solution annealed 316 SS (US shown) and 5052-O Al exhibited the greatest deviations from PLSH behavior. For all the alloys, PLSH was observed during the deformation preceding necking, and n was therefore determined from the slope of a straight line fit to this portion of a log–log trace. The true uniform elongation was calculated from the engineering value of the uniform elongation using the equation $\epsilon_u = \ln(1 + e_u)$. The standard deviation in the true uniform elongation was less than or equal to $\pm 6\%$ of the average value.

3. Results and discussion

3.1. Comparison of strain hardening exponent and true uniform elongation

PLSH theory predicts that n and ϵ_u should be equal. Fig. 2 shows that for the materials, tensile specimen geometries, and measurement technique used in the

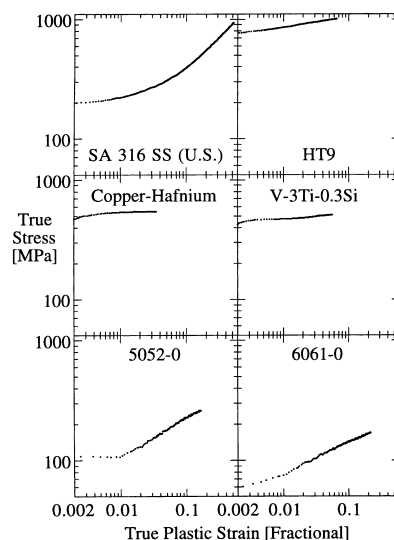


Fig. 1. Selected log–log plots of true stress vs. true plastic strain for the materials examined.

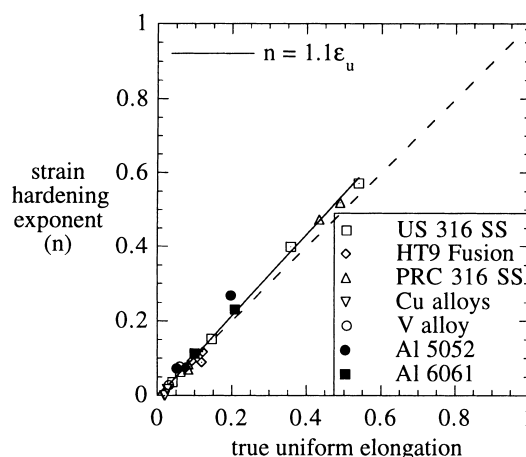


Fig. 2. Measured strain hardening exponent plotted vs. the measured true uniform elongation.

current work, a linear relationship, which is nearly 1:1, exists between the measured strain hardening exponent and the true uniform elongation.

3.2. Strain hardening exponent predicted from tensile tests

Before comparing n to n_τ, n_σ as determined from Eq. (3) was first compared to n . If the materials were to exhibit PLSH behavior over the entire range of plastic deformation, then a 1:1 relationship would exist between n and n_σ . Since the materials exhibited PLSH behavior over only a limited range of plastic deformation, it was suspected that a 1:1 relationship between n and n_σ would

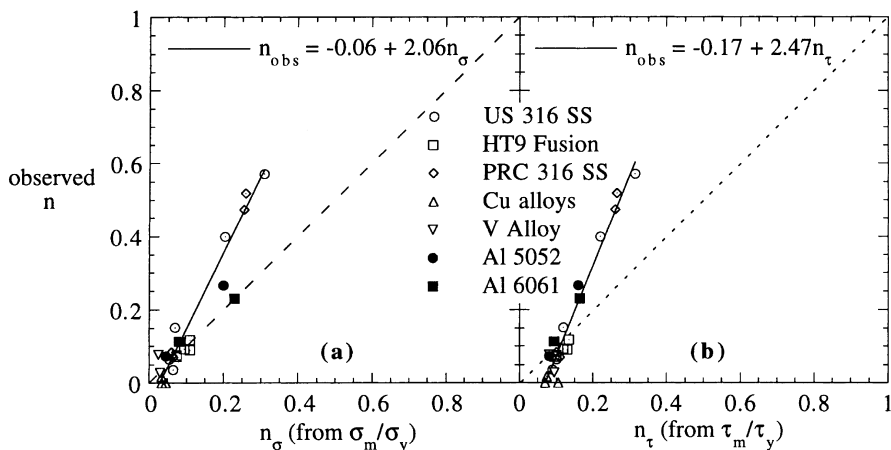


Fig. 3. Measured value of n plotted vs. either n_σ or n_τ . Materials which deviated most strongly from the 1:1 relationship also showed the greatest deviation from PLSH behavior.

not exist. n plotted as a function of n_σ is shown in Fig. 3(a), and it can be seen that while the relationship is not 1:1, it is nonetheless linear. The solution annealed aluminum alloy data points are thought to deviate from the linear relationship because of biaxial loading conditions brought about by a high ratio of gauge width to gauge thickness (10:1) [8,10].

3.3. Strain hardening exponent predicted from shear punch tests

While the comparison between n and n_σ shown in Fig. 3(a) does not follow the theoretically expected relationship, the data clearly show a useful linear trend. On this premise, n_τ was determined from Eq. (3) by using τ_m/τ_y instead of σ_m/σ_y . The relationship obtained between n and n_τ is shown in Fig. 3(b). The slope and

intercept of the linear regression for n vs. n_τ are similar to that for the n vs. n_σ linear regression. Plotting σ_m/σ_y against τ_m/τ_y , as in Fig. 4, shows that a nearly 1:1 relationship exists between σ_m/σ_y and τ_m/τ_y . The quality of the n vs. n_τ regression (Fig. 3(b)) is generally better than the quality of the n vs. n_σ regression (Fig. 3(a)) as evidenced by the reduced scatter of the data points around the regression line at lower values of n in Fig. 3(b). Unlike the values for n_σ , the values for n_τ from the solution annealed aluminum alloys were consistent with the linear trend.

Since many metals do not follow PLSH behavior, ϵ_u is a more useful parameter than n , and so the relationship between ϵ_u and n_τ was also examined. Fig. 5 shows the plot of ϵ_u vs. n_τ , and again, a linear relation exists

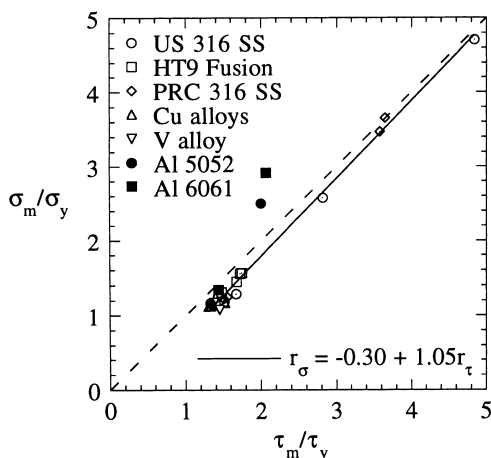


Fig. 4. σ_m/σ_y plotted vs. τ_m/τ_y .

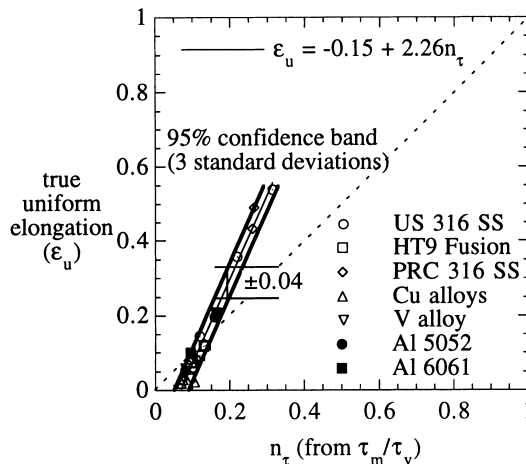


Fig. 5. Measured true uniform elongation plotted vs. n_τ . Within the 95% confidence interval, the uncertainty in the predicted value of the true uniform elongation is ± 0.04 (fractional).

between ε_u and n_τ . The quality of the regression is better than that for the n vs. n_τ plot. The magnitude of the scatter around the regression line appears to be independent of the value of ε_u . Within the 95% confidence interval (three standard deviations), the uncertainty in the value of ε_u that would be predicted from the regression is ± 0.04 .

4. Conclusions

The current work extends the original work [1] on ductility estimates from shear punch tests to a maximum strain hardening exponent of ~ 0.6 . A single, useful linear relationship was found to exist between n and n_τ for a variety of materials. By extending the maximum strain hardening exponent to ~ 0.6 , it was determined that the relationship between n and n_τ is linear but not 1:1. This behavior is due to the materials not strictly obeying PLSH behavior. It was also found that ε_u is linearly related to n_τ , permitting direct estimates of ε_u from shear punch tests. The best correlation was obtained when comparing ε_u to n_τ .

Acknowledgements

This work was supported by the Office of Fusion Energy Sciences, US Department of Energy under Contract DE-AC06-76RLO 1830.

References

- [1] G.E. Lucas, G.R. Odette, J.W. Sheckard, The Use of Small-Scale Specimens for Testing of Irradiated Material, ASTM STP 888, 1986, p. 112.
- [2] M.L. Hamilton, M.B. Toloczko, G.E. Lucas, Miniaturized Specimens for Testing of Irradiated Materials, IEA International Symposium, Forschungszentrum Jülich GmbH, 1995, p. 46.
- [3] G.L. Hankin, M.B. Toloczko, K.I. Johnson, M.A. Khaleel, M.L. Hamilton, F.A. Garner, R.W. Davies, R.G. Faulkner, Effects of Radiation on Materials: 19th International Symposium, ASTM STP 1366, 1999, p. 1018.
- [4] APT materials safety experiments technical report, LA-UR-93-2850, September 1993.
- [5] M.B. Toloczko, master's thesis, Department of Chemical and Nuclear Engineering, University of California at Santa Barbara, 1996.
- [6] F. Garafalo, F. Von Gemmingen, W.F. Domis, Trans. ASM 54 (1961) 430.
- [7] M.L. Hamilton, M.B. Toloczko, D.J. Edwards, W.F. Sommer, M.J. Borden, J.A. Dunlap, J.F. Stubbins, G.E. Lucas, Effects of Radiation on Materials, Proceedings of the 17th International Symposium, ASTM STP 1270, 1996, p. 1057.
- [8] J.A. Dunlap, M.J. Borden, W.F. Sommer, J.F. Stubbins, Effects of Radiation on Materials, Proceedings of the 17th International Symposium, ASTM STP 1270, 1996, p. 1047.
- [9] N.F. Panayotou, S.D. Atkin, R.J. Puigh, B.A. Chin, The Use of Small-Scale Specimens for Testing of Irradiated Material, ASTM STP 888, 1986, p. 201.
- [10] S. Stören, J.R. Rice, J. Mech. Phys. Solids 23 (1975) 421.